ELECTRICAL PROPERTIES OF SnO$_2$-BASED VARISTOR CERAMICS WITH SOLID-PHASE AND LIQUID-PHASE SINTERING

A. V. Gaponov, I. A. Skuratovsky

Dnipro National University, 72, Gagarin Ave., Dnipro, UA–49010, Ukraine

The varistor effect takes place in SnO$_2$–Co$_3$O$_4$–Nb$_2$O$_5$–Cr$_2$O$_3$ ceramics with CaO, SrO or BaO additions prepared by solid-phase sintering and in the same ceramics with CuO, V$_2$O$_5$ or Bi$_2$O$_3$ additions prepared by liquid-phase sintering. This effect is accompanied by a humidity-sensitive effect at the low-field electrical conductivity. The latter is observed when air relative humidity increases from 10 to 93%. The lowest humidity-sensitive effect was found in the liquid-phase sintering samples. For the investigated samples the values of the nonlinearity coefficient 24–50 at high electric fields ($E_1 = 2.8 - 11$ kV cm^{-1}) and the humidity sensitivity coefficient $1.8 \cdot 10^3$ - $3.2 \cdot 10^5$ at low electric fields were calculated. Such properties of tin oxide based ceramics can be explained within the model of electrical conduction controlled by the grain-boundary potential barriers and the dissociative adsorption of water molecules on the samples surface. This leads to a low decrease of the intergranular potential barrier height in the humid air and an increase in the conductivity in low electric fields. At the same time in the high electric fields the barrier height decreases more intensively with an increase in the electric field and this leads to the varistor effect.

Key words: electrical properties, electrical conductivity, grain boundaries, oxides, semiconductors, ceramics.

I. INTRODUCTION

Oxide ceramics is well known as a material for the preparation of surface acoustic wave devices [1], superconductors [2], current limiters [3], catalysts [4], gas sensors [5], humidity sensors [6–11], varistors [12–19] etc. The tin oxide based ceramics has many low electrical resistance grains which are usually separated by the layers with high electrical resistance. The SnO$_2$-based ceramics has non-Ohmic electrical conductivity, which is caused by the potential barriers at the SnO$_2$ grain boundaries [12–19]. These are double Schottky barriers (two Schottky barriers are connected in opposite directions).

The value of electrical conductivity depends on the electric field, temperature and environmental gas. Specifically, the electrical conductivity of SnO$_2$-based ceramics is sensitive to the variation in the air relative humidity [8–12]. Depending upon the additions to the ceramic samples, the varistor or humidity-sensitive properties can prevail. Besides, the devices with combined properties of a varistor and a sensor of relative humidity can be used. For example, such ceramics were studied in the system SnO$_2$–ZnO–CoO with Bi$_2$O$_3$, SiO$_2$ or GeO$_2$ additions [12] or in the system SnO$_2$–Co$_3$O$_4$–Nb$_2$O$_5$–Cr$_2$O$_3$ (SnCoNbCr) with Bi$_2$O$_3$ [20, 21], V$_2$O$_5$ [22] or CuO [23] additions. The combining of both properties in SnCoNbCr ceramics with different additions is due to the grain-boundary nature of both effects [20–23]. All additions in the latter system have low melting temperatures, which are less than burning temperature. Therefore, those ceramics have liquid phases in the process of sintering.

Recently, we have found that other additives (CaO, SrO or BaO) to tin dioxide can provide varistor and sensor effects (nonlinearity coefficient $\beta \approx 30$-50, humidity sensitivity coefficient $S \approx 10^4$-10^5). These systems have no liquid phases at sintering, but have intergranular inclusions. The behavior of these ceramic materials under various humidity conditions is very important for the varistor application.

To study the effect of different oxides on the electrical properties including humidity sensitivity of SnO$_2$-based varistor ceramics, we investigated the SnCoNbCr system with CaO, SrO or BaO additions (solid-phase sintering) and CuO, V$_2$O$_5$ or Bi$_2$O$_3$ additions (liquid-phase sintering). The received results are presented in this paper below.

II. EXPERIMENTAL DETAILS

The samples on the basis of SnO$_2$ with (mol.%) 0.5Co$_3$O$_4$, 0.05Nb$_2$O$_5$, 0.05Cr$_2$O$_3$ addition and 0.5mol.% CaCO$_3$, SrCO$_3$, BaCO$_3$, CuO, V$_2$O$_5$ or Bi$_2$O$_3$ additions were prepared by a conventional mixture method. The pressed tablets (about 12mm in diameter and 0.75mm thick) were sintered in the air at temperature 1520K (1hour). The details of the preparation are described in [21–24]. While heating the disks with carbonates CaCO$_3$, SrCO$_3$ or BaCO$_3$, the decomposition with CO$_2$ emission took place and these compounds changed into CaO, SrO or BaO [24].

The SnO$_2$, Co$_3$O$_4$, Nb$_2$O$_5$, Cr$_2$O$_3$, CaO, SrO and BaO oxides have melting temperatures which are considerably higher than the burning temperature of ceramics (1520 K). Therefore the sintering of SnCoNbCr ceramics

and of SnO_2–Co_3O_4–Nb_2O_5–Cr_2O_3 samples with CaO, SrO or BaO additions is a solid-phase one. This conclusion is proved by the data of our previous papers [18,24]. But Bi_2O_3, V_2O_5 and CuO oxides have low melting temperatures. Therefore, ceramics with Bi_2O_3, V_2O_5 or CuO additions have Bi_2O_3-, V_2O_5- and CuO-pure intergranular layers, which are liquid at the high temperature sintering and solidify during cooling, as it was reported in our papers [20,22,23]. Thus, these samples are the liquid-phase sintering type.

Secondary electron images were obtained in the scanning electron microscope JEOL JSM-6360LV. In–Ga eutectic electrodes were used in the tested samples.

Current–voltage characteristics were recorded in dc conditions in the air with fixed relative humidity w in the 10–93% range by putting the samples into a closed chamber above the surface of the water solution of a proper salt (details are given in [22]). The temperature dependence of dc electrical conductance $\sigma(T)$ in the range of about 295–425 K was obtained by heating the samples in the air (details are given in [22–24]).

The parameters of the samples (the linear shrinkage γ, the nonlinearity coefficient β and the breakdown electric field E_1 at current density $1\,mA\cdot cm^{-2}$, the electrical conductivity σ at the low electric field, the activation energy of electrical conduction E_σ, the dielectric permittivity ε at frequency 1kHz) were calculated by the formulas given in [21–25]. The humidity sensitivity coefficient $S = \left[\sigma(w_2) - \sigma(w_1)\right]/\sigma(w_1)$ was calculated at electric field $0.5E_1$ and relative humidity $w_1 = 10\%$ and $w_2 = 93\%$ respectively.

III. RESULTS AND DISCUSSION

A. Microstructure

The obtained micrograph of the SnCoNbCr sample surface (Fig. 1a) shows that the studied ceramics contains tin dioxide grains of about 3.5μm. The material is sintered enough but nevertheless the porosity is significant. For that reason this ceramics has the environment sensitive effects.

The value of the linear shrinkage for the SnCoNbCr sample is 8.3%. CaO, SrO or BaO additions to the SnCoNbCr system lead to lower values of linear shrinkage: 6.3, 3.6 or 7.3% respectively. The relatively slight decrease of the grain size is also observed in these samples: 2.6, 1.3 or $0.8\,\mu$m respectively (Table 1). It is probably connected with the segregation of the ions with a large ion radius (104pm for Ca^{2+}, 120 pm for Sr^{2+} and 138 pm for Ba^{2+}) on the grain boundaries of SnO_2 (ion radius for Sn^{4+} 67 pm) [24] and the worsening of synthesis due to the emergence of the unfavorable conditions for the SnO_2 grain growth.
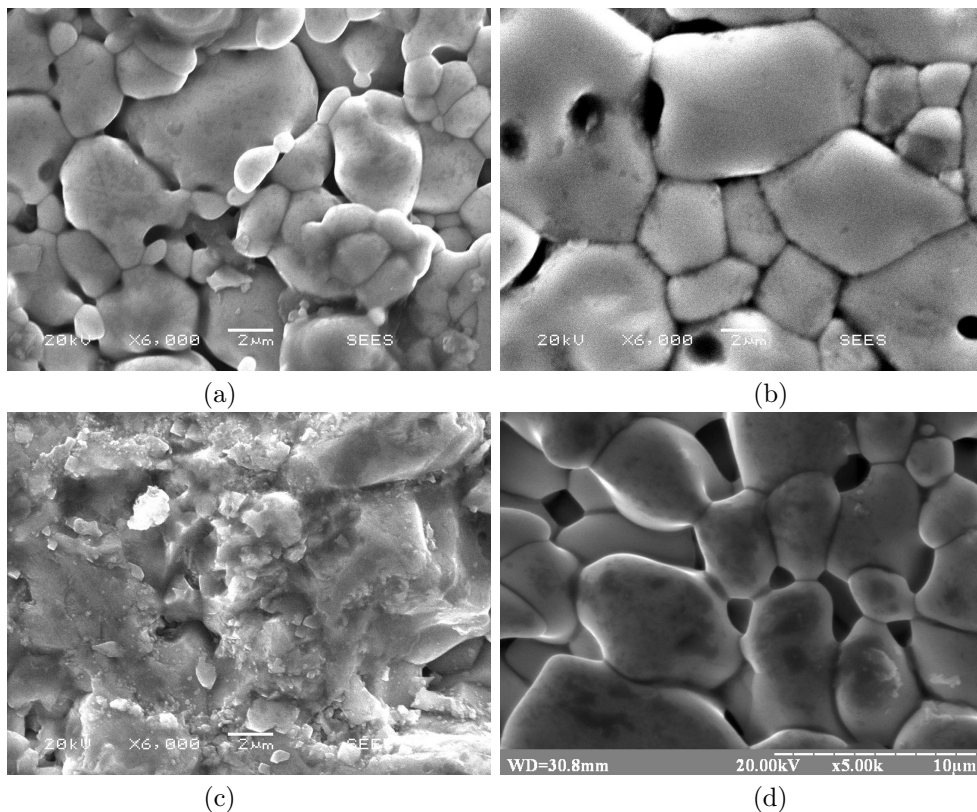

(a)

(b)

(c)

(d)

Fig. 1. Micrographs of the as-sintered surface of SnO_2–Co_3O_4–Nb_2O_5–Cr_2O_3 ceramics without (a) and with CuO (b), V_2O_5 (c) and Bi_2O_3 (d) additions.

Addition	Linear shrinkage γ, %	Average grain size l_g, μm	Humidity sensitivity coefficient S	Activation energy of electrical conduction E_σ, eV
—	8.3	3.5	$3.2 \cdot 10^5$	0.98
CaO	6.3	2.6	$2.2 \cdot 10^5$	1.04
SrO	3.6	1.3	$1.9 \cdot 10^4$	1.19
BaO	7.3	0.8	$8.5 \cdot 10^3$	0.93
CuO	10.9	5.8	$1.8 \cdot 10^3$	0.91
V_2O_5	12.2	3.2	$8.9 \cdot 10^3$	0.92
Bi_2O_3	17.0	6.0	$7.3 \cdot 10^3$	1.03

Table 1. Some parameters of SnO_2–Co_3O_4–Nb_2O_5–Cr_2O_3 ceramics with different additions.

The micrographs of ceramics with CuO, V_2O_5 or Bi_2O_3 additions are presented in Figures 1b, 1c or 1d respectively. In these figures, the surface of SnO_2 grains, that is covered by the secondary phases (especially with the V_2O_5 addition), is shown. These CuO-, V_2O_5- and Bi_2O_3-rich grain boundaries phases occur rather inhomogeneously throughout such samples. They locate in a space between the grains and even cover the grains surface of the investigated materials.

The addition of CuO, V_2O_5 or Bi_2O_3 oxides to the SnCoNbCr system causes an increase in linear shrinkages up to 10.9, 12.2 or even 17.0% respectively (Table 1). The liquid-phase sintering can lead to an increase in the linear shrinkage and the formation of a more solid and less porous structure of the obtained materials. All these effects were observed in the studied samples (Fig. 1). Thus, ceramics with CuO, V_2O_5 or Bi_2O_3 additions are the liquid-phase sintering type. This fosters grain growth at high temperatures in the process of sintering. Therefore, the average grain size in such samples is slightly bigger than for the SnCoNbCr ceramics except the sample with the V_2O_5 addition (Table 1). The V_2O_5-pure intergranular layers are randomly distributed throughout the sample and inhibit the growth of grains in such ceramics [22].

The structural features of the examined samples must be correlated with their electrical properties. The appearance of different intergranular inclusions and layers during the sintering can change the formation of potential barriers at the SnO_2 grain boundaries. So, the electrical characteristics of the studied ceramics are investigated and presented below.

B. Current–voltage characteristics and electrical parameters

Current–voltage characteristics of SnO_2-based ceramics with different additions measured in the air with relative humidity 10% are presented in coordinates $j - E$ in Fig. 2. The obtained electrical parameters of these ceramics are reported in Table 2. The $j(E)$ characteristic of the SnCoNbCr sample is highly nonlinear (Fig. 2, curve 1) with the values of nonlinearity coefficient $\beta = 49$ and electric field $E_1 = 5630$ V cm^{-1}. The relative dielectric permittivity $\varepsilon = 273$ of this sample is quite high due to the formation of the sufficiently large grains and the existence of thin depletion layers at the grain boundaries [14, 17].
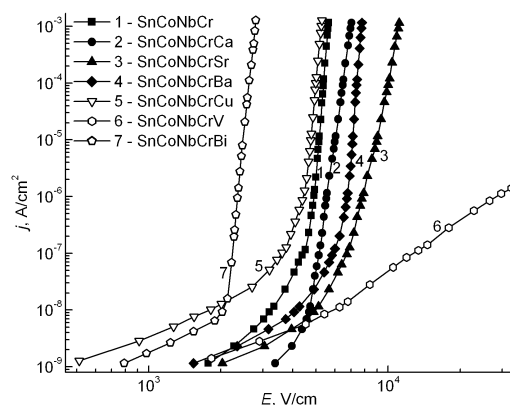
Fig. 2. Current density vs. electric field in the air with relative humidity 10% of SnO_2–Co_3O_4–Nb_2O_5–Cr_2O_3 ceramics without (1) and with CaO (2), SrO (3), BaO (4), CuO (5), V_2O_5 (6) and Bi_2O_3 (7) additions.

Addition	Nonlinearity coefficient β	Electric field, E_1, V cm^{-1}	Dielectric permittivity ε	Electrical conductivity σ, Ohm^{-1} cm^{-1}
—	49	5630	273	$6.5 \cdot 10^{-13}$
CaO	30	7000	77	$3.4 \cdot 10^{-13}$
SrO	24	11070	27	$5.7 \cdot 10^{-13}$
BaO	50	7750	138	$7.5 \cdot 10^{-13}$
CuO	42	5260	485	$2.5 \cdot 10^{-12}$
V_2O_5	2.9*	28280*	14	$7.7 \cdot 10^{-13}$
Bi_2O_3	45	2790	470	$1.5 \cdot 10^{-12}$

*at j = 10^{-6} A cm^{-2}

Table 2. Electrical parameters of SnO_2–Co_3O_4–Nb_2O_5–Cr_2O_3 ceramics with different additions with air relative humidity 10%.

The addition of alkaline earth oxides leads to some increase in electric field E_1 (Fig. 2, curves 2–4) though the values of nonlinearity coefficient β remain quite high (Table 2). The sample with CaO addition has a slightly smaller value $\beta = 30$ at the increase in E_1 up to $7000\,V\,cm^{-1}$. The addition of SrO causes the highest value of $E_1 = 11070\,V\,cm^{-1}$. The sample with BaO addition has a rather large value of the nonlinearity coefficient $\beta = 50$. The observed increase in the electric field E_1 in the samples with CaO, SrO or BaO additions (Table 2) is due to the decrease of the average grain size l_g (Table 1) and to the increase in the number of grain boundaries per unit length correspondingly. The values of relative dielectric permittivity of the samples ε are also correlated with the sizes of SnO$_2$ grains. Therefore, the values of dielectric permittivity are smaller for the ceramics with CaO, SrO or BaO additions (Table 2).

In the ceramics with CuO or Bi$_2$O$_3$ additions, the electric field E_1 is weaker (Fig. 2, curves 5 and 7) than for the SnCoNbCr sample because the grain sizes in these ceramics are larger (Table 1). Therefore, the dielectric permittivities of the samples with CuO or Bi$_2$O$_3$ additions are larger than those of the SnCoNbCr ceramics (Table 2). Ceramics with CuO addition exhibits a little bit smaller value of nonlinearity coefficient $\beta = 42$. Probably, the tin oxide grains are not wetted enough by the CuO-pure secondary phases (see Fig. 1b), and therefore the Co$_3$O$_4$ and Cr$_2$O$_3$ oxides are nonuniformly distributed on the sample. These additions are responsible for the formation of the high potential barriers at the SnO$_2$ grain boundaries [14, 17]. Consequently, these potential barriers are insufficiently high and the nonlinearity of the sample current–voltage characteristics is not high enough. Therefore, the improvement of the ceramics structure homogeneity is one of the most important tasks in the process of the high-quality varistor development. The sample with Bi$_2$O$_3$ addition has a slightly smaller value of nonlinearity coefficient $\beta = 45$ than the SnCoNbCr sample (Table 2). This effect is observed at the transition from high-voltage to low-voltage SnO$_2$-based ceramics [16, 26].

The V$_2$O$_5$ addition to the SnCoNbCr ceramics causes a significant decrease of the nonlinearity coefficient and an increase in the breakdown electric field (Fig. 2, curve 6). The vanadium oxide forms quite conductive V$_2$O$_5$-pure intergranular phases, which cover SnO$_2$ grains (Fig. 1c) and works as an electric shunt to the grain boundaries [22]. Therefore, the nonlinearity of current–voltage characteristics became considerably lower and it became impossible to reach electric field E_1 (at $1\,mA\,cm^{-2}$) under our experiment conditions. Besides, the sample with V$_2$O$_5$ addition exhibits lower $\varepsilon = 14$ due to the influence of the vanadium oxide phase with low relative dielectric permittivity [27, 28].

The current–voltage characteristics of the studied SnO$_2$-based ceramics contain two regions. The first is Ohmic and low-nonlinear part at low currents and voltages, and the second is high-nonlinear part at high currents and voltages (Fig. 2). In SnCoNbCr ceramics, the high-nonlinear part of $j(E)$ characteristic is initiated at

current density $j \approx 1 \cdot 10^{-6}\,A\,cm^{-2}$ (Fig. 2, curve 1). This material has relatively high low-field electrical conductivity σ. The values of electrical conductivity σ became larger with the addition of CuO or Bi$_2$O$_3$ oxides to the ceramics (Table 2). In such samples, the average SnO$_2$ grain size is larger than that in the SnCoNbCr sample (Table 1). It leads to a decrease of the number of grain boundaries and potential barriers per length unit. Consequently, the electrical conductivity σ increases.

The certain decrease of low-field conductivity is observed in the case of CaO addition (Fig. 2, curve 2). That sample has the lowest value $\sigma = 3.4 \cdot 10^{-13}\,Ohm^{-1}\,cm^{-1}$ (Table 2). This effect is connected with the decrease of the grain size (a significant decrease of the grain boundary cross-section, the increase of grain neck resistivity) and the increase of the height of the grain boundary potential barriers (see later about this). The effect with the lowered low-field conductivity is reproducible if the relative humidity of the air increases. In the air with higher relative humidity, the sample with CaO addition also has the lowest electrical conductivity.

The high nonlinearity of current–voltage characteristics in the studied ceramics with the nonlinearity coefficient $\beta = 24 - 50$ is rather attributed to the grain-boundary nature of the conduction mechanism for different SnO$_2$-based varistors [12–24, 26]. Electrical conduction in ceramic samples exists across electrically active grain boundaries. In these ceramics, the grains are quite conductive but grain-boundary regions are resistive due to the formation of grain-boundary potential barriers during the sintering of the ceramic samples in oxidizing atmosphere. The existence of the grain-boundary barriers in the studied samples is confirmed by the following observed facts: (a) thermally-activated electrical conduction; (b) strong non-Ohmic conduction at relatively low electric fields; (c) reversible increase of capacitance with an increase in relative humidity.

The model of non-Ohmic conduction in SnO$_2$-based ceramics takes into account the decrease of the grain-boundary double Schottky barrier height with an increase in the electric field [18, 19, 26]. The increase in the voltage applied to a SnO$_2$-based varistor can lead to a rather slight decrease of the barrier height at low voltages because the trapping of electrons at the grain-boundary interface states prevents from quick decrease of the barrier height. Then the barrier height decrease is rather stronger at higher voltages [18,19,26]. The physics of such voltage dependence of the barrier height in SnO$_2$-based varistors can be similar to the situation in ZnO-based varistors [29,30]. The electrons are tunneling in the conduction band across the barrier if the barrier height is decreasing due to the appearance of holes (minority carriers) near the grain boundary of n-type semiconductor [29].

C. Temperature dependences of electrical conductivity

The different additions to SnO$_2$-based systems can modify the conditions of the grain-boundary potential

barrier formation. To explain the observed alteration of the low-field conductivity in the samples with different additions, the temperature dependences of dc electrical conductivity $\sigma(T)$ were studied (Fig. 3). The obtained values of the activation energy of electrical conduction E_σ for the investigated SnO_2-based ceramics are presented in Table 1.
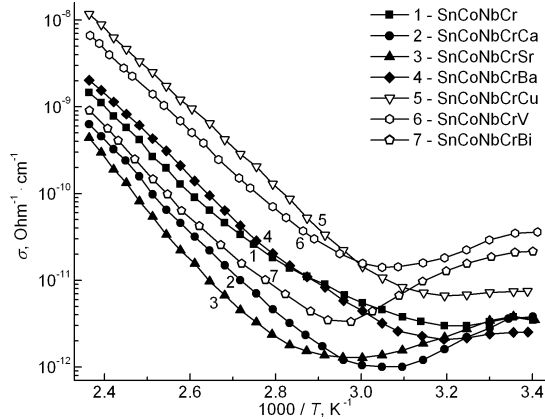

Fig. 3. Temperature dependences of electrical conductivity of SnO_2–Co_3O_4–Nb_2O_5–Cr_2O_3 ceramics without (1) and with CaO (2), SrO (3), BaO (4), CuO (5), V_2O_5 (6) and Bi_2O_3 (7) additions.

All $\sigma(T)$ dependences are quite complicated: they cannot be approximated by a straight line in the whole studied temperature range 295–425 K (Fig. 3). At low temperatures, in the range of about 295–330 K, the decrease of conductivity during the heating is caused by the desorption of water molecules [20–23]. The humid air at room conditions can penetrate inside the samples and reach grain-boundary regions. During the heating, water molecules evaporate and electrical conductivity decreases (Fig. 3). Further temperature growth from about 330 to 425 K causes a thermally-activated increase in conductivity.

The obtained $E_\sigma \approx 1$ eV of the SnCoNbCr sample gives a correct estimation of the barrier height [25]. The addition of different oxides leads to some variation in $\sigma(T)$ dependences (Fig. 3). Generally, the values of activation energy are quite high ($E_\sigma \approx 0.9 - 1.2$ eV). The slight decrease of E_σ is found for the ceramics with BaO, CuO or V_2O_5 additions (Table 1). It causes the increase in low-field electrical conductivity in these samples (Fig. 2). With adding CaO, SrO or Bi_2O_3 in the SnCoNbCr ceramics, the activation energy slightly increases (Table 1), which leads to a decrease of electrical conductivity in low electric field (Fig. 2). Such behavior is not observed in the sample with the Bi_2O_3 addition due to the larger value of the average SnO_2 grain size (Table 1) and the smaller number of grain boundaries per unit length accordingly.

Thus, in the SnCoNbCr sample and in the ceramics with different additions, electrical conductivity is controlled by the grain-boundary potential barriers. The thermionic emission across the barrier is the most probable conduction mechanism near about 300K. Electrical properties of the studied ceramics are dependent on the microstructure and on the potential barrier height. The

smaller the barrier height is, the larger the electrical conductivity in the low field is, and vice versa.

D. Effect of humidity on the electrical properties

Low-field electrical conductivity of various SnO_2-based ceramics ncreases with the growth of air relative humidity [8–12, 20–23]. However, the humidity sensitivity of solid-phase sintering and liquid-phase sintering ceramic samples is studied insufficiently. Therefore, we decided to study current–voltage characteristics of all obtained materials under different humidity conditions.

For SnCoNbCr ceramics, the $j(E)$ dependences measured in the air with different relative humidity are close to linear in low fields but they are highly nonlinear in higher fields [22]. The rise in relative humidity from 10 to 93% causes a strong shift of low-field part of $j(E)$ characteristics to higher current but high-field part of these characteristics changes slightly. This effect is reversible and reproducible. If the sample is placed in a dry air chamber (with relative humidity 10%) after a humid air chamber (with relative humidity from 34 to 93%), then its characteristics return to the initial state.
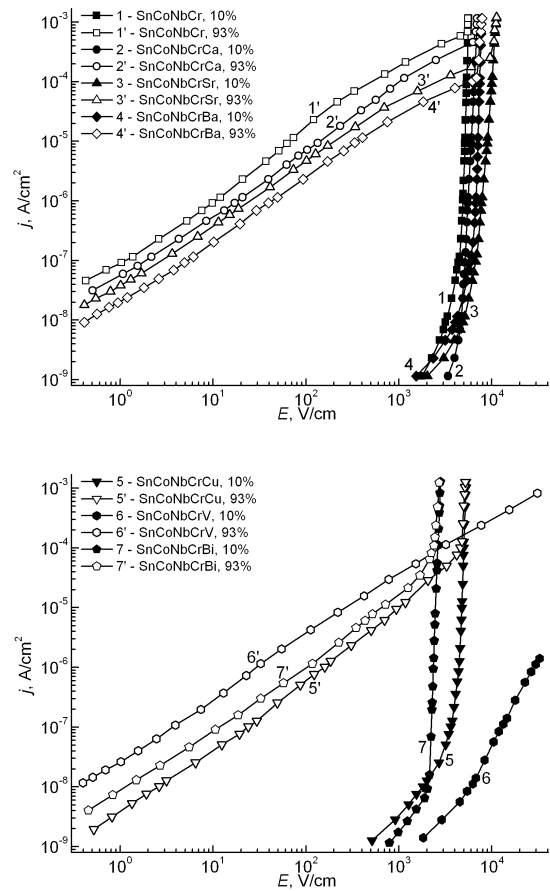

Fig. 4. Current density vs electric field of SnO_2–Co_3O_4–Nb_2O_5–Cr_2O_3 ceramics without $(1, 1')$ and with CaO $(2, 2')$, SrO $(3, 3')$, BaO $(4, 4')$, CuO $(5, 5')$, V_2O_5 $(6, 6')$ and Bi_2O_3 $(7, 7')$ additions in the air with relative humidity 10% $(1–7)$ and 93% $(1' - 7')$.

That phenomenon is observed for all the materials studied in our paper. In Fig. 4, we present j(E) dependencies of SnO_2-based ceramics in the air with relative humidity 10 and 93%. The rise in relative humidity causes an increase in the low-field samples conductivity. It increases less in the sample with CuO addition than in other samples. The intergranular layers of CuO secondary phases prevent the access of the humid air into the electrically active regions of grain boundaries and diminish the role of the barrier-related sensitivity mechanism.

In order to estimate the effect of humidity on the ceramics characteristics, the values of the humidity sensitivity coefficient S are presented in Table 1. For the solid-phase sintering samples with the additions of alkaline earth metal oxides, an increase in ion radius elements from Ca^{2+} (104 pm) to Ba^{2+} (138 pm) causes a gradual decrease of the S values. It can be explained by the segregation of the secondary solid phases at the grain boundaries [24] and the decrease of the environmental influence on the electrical properties of the ceramics. For the liquid-phase sintering samples with CuO, V_2O_5 or Bi_2O_3 additions the humidity sensitivity is smaller (Table 1) because such ceramics is more solid and less porous. Besides, solidified at sintering, the CuO, V_2O_5 or Bi_2O_3 secondary phases (see Fig. 1b, 1c, 1d respectively) cover the surface of SnO_2 grains or only grain-boundary regions and partially prevent the penetration of humid air into the grain boundaries. As a result, the electrical conductivity increases less at a higher humidity. Therefore, the humidity sensitivity of the ceramics that were prepared by liquid-phase sintering is lower than that of ceramics that were prepared by solid-phase sintering.

The high humidity sensitivity of the studied material is explained by the grain boundary controlled conduction mechanism [12, 20–23]. The potential barriers of SnO_2 grain boundary are formed during the sintering of the ceramics in the air [12–24, 26]. The observed increase in the low-voltage electrical conductivity with the rise in the air relative humidity (Fig. 4) can be explained by the decrease of the barrier height. It was shown that the barrier height decreases by only about 20% if the air relative humidity reaches about 80% [21]. Therefore, the potential barriers of the grain boundaries at a high humidity are still sufficiently high to be decreased at high voltages. So, highly nonlinear $j(E)$ dependences are still observed at high values of relative humidity (Fig. 4).
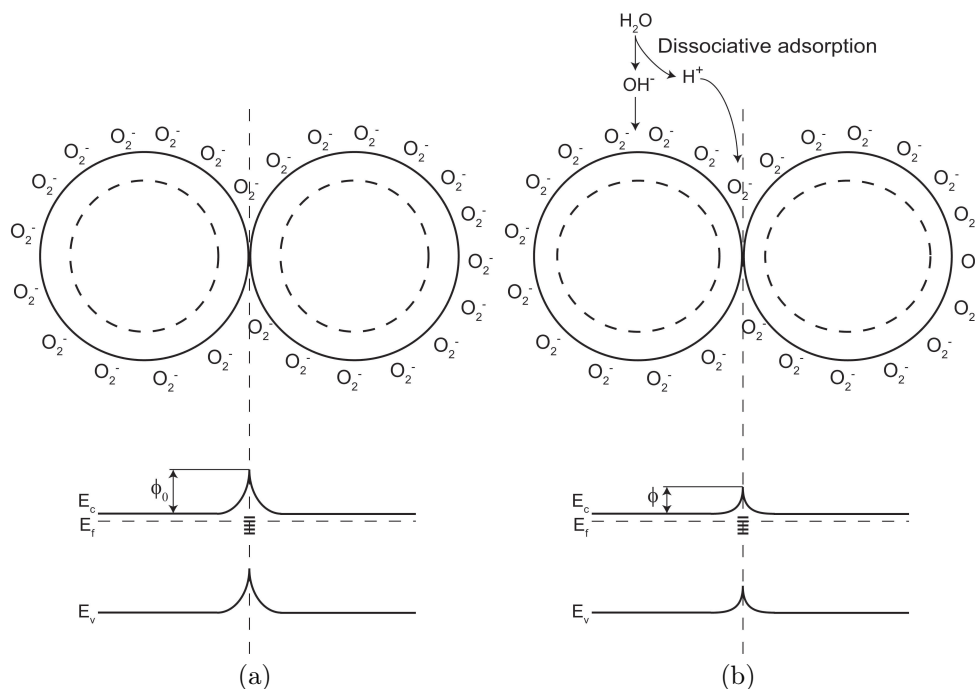

Fig. 5. The grain boundary defect model for SnO_2-based ceramics during the adsorption of water molecules in dry (a) and wet (b) air.

However, the nonlinearity of the high-field part of $j(E)$ characteristics somewhat decreases with an increase in the air relative humidity (Fig. 4). The cause of this is the increase in the surface electrical conductivity of the samples due to the adsorption of water molecules [21]. This surface conductivity shunts the non-Ohmic volume electrical conductivity and leads to some decrease of the nonlinearity coefficient β.

The adsorption of water molecules on the surface of the studied ceramics also gives rise to low-field electrical conductivity. The adsorbed water molecules can dissociate according to the reaction

$$H_2O \leftrightarrow H^+ + OH^-.$$
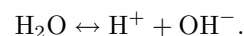
The quite mobile proton H^+ can penetrate to the region near the grain boundary and interact with the oxygen which has been chemisorbed there in the O_2^- form [31] during the sintering of the ceramics in the oxidizing

atmosphere. As a result, the total negative charge at the near-surface grain boundary can become lower in absolute value, which leads to a decrease of potential barrier height (Fig. 5). Therefore, in the air with higher relative humidity the grain-boundary potential barriers are lower at the near-surface regions of the sample and the low-field electrical conductivity of the ceramics is larger than in the air with lower value of relative humidity.

After the current–voltage characteristics had been recorded, the voltage was disconnected and the samples were placed into a dry air chamber. Here the desorption of water molecules began, during which the protons delocalized from near-surface grain boundary regions, where they had been captured in humid air. So, the potential barrier heights are increasing and the low-field electrical conductivity of the sample is decreasing. The $j(E)$ characteristics return to the initial state.

Thus, the discussed humidity-sensitive effect in tin oxide based ceramics leads to an increase in low-field electrical conductivity in humid air in comparison with the dry air conditions. The obtained SnO$_2$-based samples are materials with humidity-sensitive conductivity. They can be used as sensors for measuring the air relative humidity.

IV. CONCLUSIONS

The varistor characteristics and the humidity-sensitive properties are observed in SnO$_2$-based ceramics with different additions. These peculiarities are explained by the dependence of the grain-boundary barrier height on relative humidity (in a low electric field) and on voltage (in a high electric field) respectively. The estimated values of the barrier height of the studied samples are about $0.9 - 1.2\,\text{eV}$. The low-field electrical conductivity of SnO$_2$-based ceramics increases with a rise in the relative humidity of the air. The highest humidity sensitivity coefficient $S = 3.2 \cdot 10^5$ was obtained for SnO$_2$–Co$_3$O$_4$–Nb$_2$O$_5$–Cr$_2$O$_3$ ceramics. The values of S decrease with CaO, SrO and BaO additions (solid-phase sintering) and greatly decrease with CuO, V$_2$O$_5$ and Bi$_2$O$_3$ additions (liquid-phase sintering).The lowest value $S = 1.8 \cdot 10^3$ at high nonlinearity coefficient of $\beta = 42$ and electric field $E_1 = 5260\,V\cdot \text{cm}^{-1}$ was obtained for ceramics with CuO addition. The CaO addition provides the lowest value of low-field electrical conductivity for the studied tin oxide based varistor ceramics. The observed decrease of the low-field conductivity of SnO$_2$-based samples with different additions correlates with the experimentally found increase in the activation energy of electrical conduction and the decrease of the grain size.

[1] C. R. Gorla *et al.*, J. Appl. Phys. **85**, 2595 (1999); https://doi.org/10.1063/1.369577.

[2] V. Micevski, V. Lovchinov, Z. Milosavlevski, S. Stoimenov, J. Phys. Stud. **5**, 323 (2001).

[3] A. Bondarchuk, A. Glot, G. Behr, J. Werner, J. Phys. Stud. **11**, 408 (2007).

[4] L. Toporovska *et al.*, J. Phys. Stud. **22**, 1601 (2018); https://doi.org/10.30970/jps.22.1601.

[5] W. Gopel, K. D. Schierbaum. Sens. Actuat. B: Chem. **26**, 1 (1995); https://doi.org/10.1016/0925-4005(94)01546-T.

[6] B. M. Kulwicki, J. Am. Ceram. Soc. **74**, 697 (1991); https://doi.org/10.1111/j.1151-2916.1991.tb06911.x.

[7] M. Pelino, C. Cantalini, M. Faccio. Active Passive Elec. Comp. **16**, 69 (1994); https://doi.org/10.1155/1994/91016.

[8] E. Traversa, Sens. Actuat. B: Chem. **23**, 135 (1995); https://doi.org/10.1016/0925-4005(94)01268-M.

[9] Z. Chen, C. Lu, Sensor Lett. **3**, 274 (2005); https://doi.org/10.1166/sl.2005.045.

[10] S. P. Yawale, S. S. Yawale, G. T. Lamdhade, Sens. Actuat. A: Phys. **135**, 388 (2007); https://doi.org/10.1016/j.sna.2006.08.001.

[11] T. A. Blank, L. P. Eksperiandova, K. N. Belikov, Sens. Actuat. B: Chem. **228**, 416 (2016); https://doi.org/10.1016/j.snb.2016.01.015.

[12] A. B. Glot, Inorg. Mater. **20**, 1522 (1984).

[13] A. B. Glot, A. P. Zlobin, Inorg. Mater. **25**, 274 (1989).

[14] S. A. Pianaro, P. R. Bueno, E. Longo, J. A. Varela. J. Mater. Sci. Lett. **14**, 692 (1995); https://doi.org/10.1007/BF00253373.

[15] P. N. Santosh, H. S. Potdar, S. K. Date. J. Mater. Res. **12**, 326 (1997); https://doi.org/10.1557/JMR.1997.0046.

[16] A. B. Glot, in *Ceramic Materials Research Trends*, edited by P. B. Lin (Nova Science Publishers Inc., New York, 2007), p. 227.

[17] P. B. Bueno, J. A. Varela, E. Longo, J. Eur. Ceram. Soc. **28**, 505 (2008); https://doi.org/10.1016/j.jeurceramsoc.2007.06.011.

[18] A. B. Glot, A. V. Gaponov, A. P. Sandoval-Garcia. Phys. B **405**, 705 (2010); https://doi.org/10.1016/j.physb.2009.09.091.

[19] A. V. Gaponov, A. B. Glot, Semicond. Phys. Quant. Electron. Optoelectr. **14**, 71 (2011); https://doi.org/10.15407/spqeo14.01.071.

[20] I. Skuratovsky, A. Glot, E. Di Bartolomeo, E. Traversa, R. Polini, J. Eur. Ceram. Soc. **24**, 2597 (2004); https://doi.org/10.1016/j.jeurceramsoc.2003.09.008.

[21] I. Skuratovsky, A. Glot, E. Traversa, Mater. Sci. Eng. B **128**, 130 (2006); https://doi.org/10.1016/j.mseb.2005.11.039.

[22] A. V. Gaponov, A. B. Glot, A. I. Ivon, A. M. Chack,

G. Jimenez-Santana, Mater. Sci. Eng. B **145**, 76 (2007); https://doi.org/10.1016/j.mseb.2007.10.003.

[23] A. B. Glot *et al.*, Adv. in Tech. Mat. Mat. Proc. J. **10**, 21 (2008); https://doi.org/10.2240/azojomo0277.

[24] A. V. Gaponov, O. V. Vorobiov, A. M. Vasyliev. Phys. Chem. Solid State **17**, 81 (2016); https://doi.org/10.15330/pcss.17.1.81-87.

[25] M. Batzill, U. Diebold, Prog. Surf. Sci. **79**, 47 (2005); https://doi.org/10.1016/j.progsurf.2005.09.002.

[26] A. B. Glot, I. A. Skuratovsky, Mater. Chem. Phys. **99**, 487 (2006); https://doi.org/10.1016/j.matchemphys.2005.11.028.

[27] A. I. Ivon, I. M. Chernenko, Izv. Vyssh. Ucheb. Zaved. Fiz. **21**, 111 (1978); https://doi.org/10.1007/BF00896309.

[28] R. Sengodan, B. Chandar Shekar, S. Sathish, Phys. Proc. **49**, 158 (2013); https://doi.org/10.1016/j.phpro.2013.10.022.

[29] G. D. Mahan, L. M. Levinson, H. R. Philipp, J. Appl. Phys. **50**, 2799 (1979); https://doi.org/10.1063/1.326191.

[30] A. B. Glot, J. Mater. Sci.: Mater. Electron. **17**, 755 (2006); https://doi.org/10.1007/s10854-006-0019-y.

[31] S.-C. Chang, J. Vac. Sci. Technol. **17**, 366 (1980); https://doi.org/10.1116/1.570389.

ЕЛЕКТРИЧНІ ВЛАСТИВОСТІ ТВЕРДОФАЗНОЇ І РІДКОФАЗНОЇ СИНТЕЗОВАНОЇ ВАРИСТОРНОЇ КЕРАМІКИ НА ОСНОВІ SnO₂

О. В. Гапонов, І. А. Скуратовський

Дніпровський національний університет імені Олеся Гончара,
просп. Гагаріна, 72, Дніпро, 49010, Україна

Варисторний ефект відбувається як у SnO_2–Co_3O_4–Nb_2O_5–Cr_2O_3 кераміці з CaO, SrO або BaO доміш-ками, яка виготовлена твердофазним синтезом, так і в подібній кераміці з CuO, V_2O_5 або Bi_2O_3 домішками, яка виготовлена рідкофазним синтезом. Цей ефект супроводжувався вологочутливим ефектом для елек-тричної провідності у слабкому полі. Останній спостерігався при збільшенні відносної вологості повітря з 10 до 93%. Найменшу вологочутливість мають рідкофазні синтезовані зразки. Для досліджених зразків обчислені значення коефіцієнта нелінійності 24–50 за сильних електричних полів ($E_1 = 2.8 - 11$ кВ·см$^{-1}$) і коефіцієнта вологочутливості $1.8 \cdot 10^3 - 3.2 \cdot 10^5$ за слабких електричних полів. Такі властивості оксидно-олов'яної кераміки пояснюються моделлю для електричної провідності, яка контролюється потенціальними бар'єрами на межах зерен, і дисоціативною адсорбцією молекул води на поверхні зразків. Це зумовлює слабке зменшення висоти міжкристалічних потенціальних бар'єрів у вологому повітрі й збільшення провід-ності в слабких електричних полях. Водночас у сильних електричних полях висота бар'єрів зменшується інтенсивніше з підвищенням електричного поля, і це приводить до варисторного ефекту.